

The energy flux into a fluidized granular medium at a vibrating wall

Sean McNamara and Jean-Louis Barrat

Département de Physique des Matériaux

Université Claude Bernard and CNRS, 69622 Villeurbanne Cedex, France

(February 28, 2018)

Abstract

We study the power input of a vibrating wall into a fluidized granular medium, using event driven simulations of a model granular system. The system consists of inelastic hard disks contained between a stationary and a vibrating elastic wall, in the absence of gravity. Two scaling relations for the power input are found, both involving the pressure. The transition between the two occurs when waves generated at the moving wall can propagate across the system. Choosing an appropriate waveform for the vibrating wall removes one of these scalings and renders the second very simple.

One of the essential differences between fluidized granular systems and usual gases is that sustaining a fluidized state necessitates a continuous input of energy into the system, since the particle kinetic energy is dissipated during the collisions. Experimentally, this is often achieved by using a vibrating piston. The nature of the energy exchange between the vibrating piston and the fluidized granular medium, however, does not appear to have been studied in great detail. In most cases, it is assumed that the vibrating wall imposes a “granular temperature” of the particles that corresponds to its mean squared velocity. The purpose of this work is to achieve a more detailed understanding of this energy exchange by studying numerically and theoretically a particularly simple case. The system we consider (figure 1a) is a two dimensional fluid of inelastic hard discs, contained between two walls in the y direction and with periodic boundary conditions in the x direction. The moving wall is, at its lowest point, at $y = 0$, while a stationary wall limits the system at $y = H$. For the sake of simplicity, we have chosen to treat the wall/particle collisions as elastic, and to set the gravity force equal to zero. Hence the system can be entirely characterized by a small number of dimensionless parameters. These parameters are the ratios of the system sizes H (in the y direction) and L (in the x direction) to the particle radius a , the density measured by the area fraction $N\pi a^2/LH$ (N is the number of particles), the amplitude of vibration A of the moving wall, measured in units of a , and the restitution coefficient $r < 1$. [In the center of mass frame of two colliding particles $v'_n = -rv_n$, where v_n (v'_n) is the normal component of the particles’ velocity before (after) the collision.] Finally, the problem is completely defined by specifying the waveform $\phi(t)$ of the wall vibration. Note that τ , the period of this waveform defines the time unit in the problem. There is a second timescale in the problem: t_{coll} , the time between collisions experienced by an average particle. But t_{coll} is not independent of τ ; the ratio τ/t_{coll} is a function of the five dimensionless numbers given above. In the simulations considered here, $2 \leq \tau/t_{\text{coll}} \leq 40$. In figure 1b, we show the two waveforms, labeled (A) and (B), used to drive the vibrating wall.

We note that the system studied in this paper is an externally driven version of the system considered in references [1–3]. Despite its simplicity, this system was shown to display a

nontrivial behavior even in the absence of external forcing, with the development of several instabilities during “homogeneous cooling”. Other instabilities, such as the formation of lateral structures in the x direction, could be expected in the forced case. Since our main object is the study of energy input at a local scale, we deliberately avoided such structures by using a relatively small system width, $L/a = 50$.

If we were to add gravity to the system studied in this paper, we would have the system studied in references [4,5]. These references present discrepancies between theory and experiment which could be resolved by insights presented in this paper.

Figure 2 shows that a detailed understanding of the particle-wall interaction is needed. When the wall is driven with the asymmetric wave form (B), the relation between the average energy per particle E/N and the restitution coefficient obeys a simple power law $E/N \sim (1 - r)^{-1.9}$. On the other hand, the symmetric waveform (A) generates much more complicated behavior. Since the only difference between these two curves is the waveform, their differences cannot be explained without understanding what happens at the vibrating boundary. This paper explains how the waveform causes the two different relations between E/N and r .

We begin by looking closely at what is happening inside the system. We show typical density and temperature profiles in figure 3, for a system driven by a symmetric waveform (type (A) in figure 1b). The evolution of the profiles during the wall motion is also detailed in these figures. As the vibrated system is “heated” by the moving wall, an inhomogeneous density and temperature (temperature being understood here as kinetic energy per particle) profile develops. Far from the moving wall, the system is denser and cooler than close to it. The temperature profile clearly displays two different regions. In a region that extends over about half the height H of the box, a heat pulse generated at the vibrating wall propagates in the positive y direction. Farther away from the moving wall, the heat pulses are completely damped and the temperature is stationary. The “boundary region” for the temperature thus appears to be rather broad. The density profile also displays a (small) time dependent component, indicating that the heat pulses are coupled to compression waves

in the fluid. These heat and density waves can transport significant amounts of energy within the boundary region. This is in conflict with the assumption that energy transport is dominated everywhere by conduction (for example in [6]). We note that similar waves have been seen in simulations of shaken granular materials under gravity [7]. These waves resemble sound waves in a gas. However, their description in terms of a single “temperature” is not perfectly accurate. A more careful examination shows that the particles in these waves can be divided into two distinct populations with significantly different kinetic temperatures. One population is made up of rapidly moving particles who, having just encountered the moving wall, travel towards the stationary region, carrying the heat pulses. The other is a population of slowly moving particles emerging from the stationary region, and traveling towards the moving wall.

As r is increased towards 1, these pulses broaden, and they penetrate farther into the stationary region. Eventually, they reach the stationary wall, so that the boundary region extends to the whole simulation box.

We now seek a law giving the power injected by the wall, P_w in terms of the kinetic pressure p (defined as the momentum transfer to the stationary wall per unit surface and time). Because of momentum conservation, the pressure on the vibrating wall must also be p , and dimensional reasoning suggests that the power input should be proportional to p times the wall velocity V . For the asymmetric waveform (B), this proportionality is indeed easily shown to hold as an equality. The argument is as follows. Collisions between the particles and the wall take place only when the wall is in its ascending phase. When such a collision takes place, the energy change and the momentum change of the particle are related by $\Delta E = V\Delta p_y$. Summing over all particles that hit the wall during a cycle shows that the average energy transfer per unit time will be equal to the wall velocity multiplied by the momentum transfer per unit time, i.e. $P_w = pVL$. This conclusion is extremely well borne out by the simulation results, as can be seen in figure 4.

The reasoning can be generalized to the case of other waveforms, e.g. (A). In that case, the particles can either receive or lose energy as they hit the wall. If the arrival times of

the particles at the vibrating wall are independent of the phase of the vibrating wall, then the probabilities of these two events will depend only on the ratio between velocity of the particles and the wall velocity V , so that we expect the power input to scale as $pVL F(V/U)$, where U is a velocity characteristic of the particles that hit the wall, and F is a dimensionless function that will depend on the waveform and of the velocity distribution of the particles near the wall. In figure 4, this scaling relation was tested by plotting the power input as a function of the dimensionless variable V/U , where the typical particle speed U is estimated by the square root of the average energy per particle, $(E/N)^{1/2}$. The unscaled values of P_w range over four orders of magnitude, so the success of the scaling is impressive. The scaling is very well obeyed except for the largest amplitudes of wall vibration, in which case it fails for small values of the rescaled power input P_w/pVL .

This failure of the scaling relationship can be traced back to the establishment of the second situation mentioned above, namely that in which the “boundary” region extends over the whole simulation cell. The transition to this situation is observed for values of the restitution coefficient very close to one and for large vibration amplitudes, and only in the case where the excitation is of the form (A). When this transition takes place, the points in figure 4 leave the scaling curve, displaying a discontinuous and nonmonotonous behavior. The reason for this behavior can be understood as follows. The heat pulse and associated compression wave now reach the upper elastic wall before disappearing. They are reflected at this wall, and eventually hit the moving wall again. The arrival times of the particles at the moving wall are no longer independent of the phase of the wall vibration, so that the simple assumptions used in deriving the scaling relationship break down. Moreover, when the energy input takes place by such a correlated collision mechanism, a nonmonotonic behavior can be understood as a resonance between the travel time of the wave and the period of wall motion.

This physical picture suggests a second scaling relationship. In figure 5, we show that $P_w = (pV^2\tau L/H) G[U\tau/(H-A)]$, where G is another dimensionless function. (The inclusion of the period of the wall vibration τ is required dimensionally.) This second scaling is valid

everywhere the first one fails. It can be understood by considering the propagation of sound waves in the box. The wave speed scales as U , so $U\tau/(H - A)$ is the fraction of the box that a wave can travel during one period. For particular values of $U\tau/(H - A)$, resonance between the wall and the waves will occur. P_w will scale as $\hat{p}VL$, where \hat{p} is the pressure amplitude of the wave. Examining the properties of sound waves in a compressible gas at pressure p , we find that the pressure and velocity amplitudes are related by $\hat{p} = (k/\omega)p\hat{u}$, where \hat{u} is the velocity amplitude, k is the wavenumber of the wave, and ω is its frequency. Setting $\hat{u} \sim V$, $k \sim H^{-1}$ and $\omega \sim \tau^{-1}$ gives the scaling in figure 5.

The resonance affects the power injected by the wall only for the symmetric waveform (A), even though waves generated by the asymmetric waveform (B) can also propagate throughout the box at large A and r close to 1. The reason is that particles can either gain or loose energy with the symmetric waveform. Thus, shifting the arrival time of a large group of particles by half a period can change the sign of P_w . On the other hand, for the asymmetric waveform (B), the amount of energy gained by the particles does not depend on the phase of the wall.

The transition between the two scalings occurs at the critical value $U\tau/(H - A) \approx 0.4$. Examination of simulations made with $30 < H < 100$ confirms that this critical value remains constant. At this time, we do not have a an explanation for this critical value, nor a detailed understanding of the transition.

We believe these results to be relevant to current experimental questions. First of all, an experimental version of this system will soon be studied in microgravity [8]. Second, these results can easily be extended to experiments done in gravity by realizing that conservation of momentum requires that the pressure (the time-averaged force on the bottom plate) be the weight of the granular material: $pL = Nmg$. Finally, this work suggests that using the waveform (B) [or an experimental approximation] may simplify results, leading to a better physical understanding of granular flows.

This work was supported by the Centre National d'Etudes Spatiales. S. McNamara benefited from a Region Rhônes-Alpes visiting scientist position at the Pole Scientifique de

Modélisation Numérique of ENS-Lyon.

FIGURES

FIG. 1. (a) A sketch of the simulated system. (b) The two waveforms used to drive the vibrating wall: the symmetric waveform (A) and the asymmetric waveform (B).

FIG. 2. The average energy per particle as a function of r , showing the effect of changing the waveform of the vibrating wall. The parameters of these simulations are $L = H = 50a$, area fraction $N\pi a^2/LH = 0.25$, wall velocity $V = 8a/\tau$, and $0.8 \leq r \leq 0.998866$.

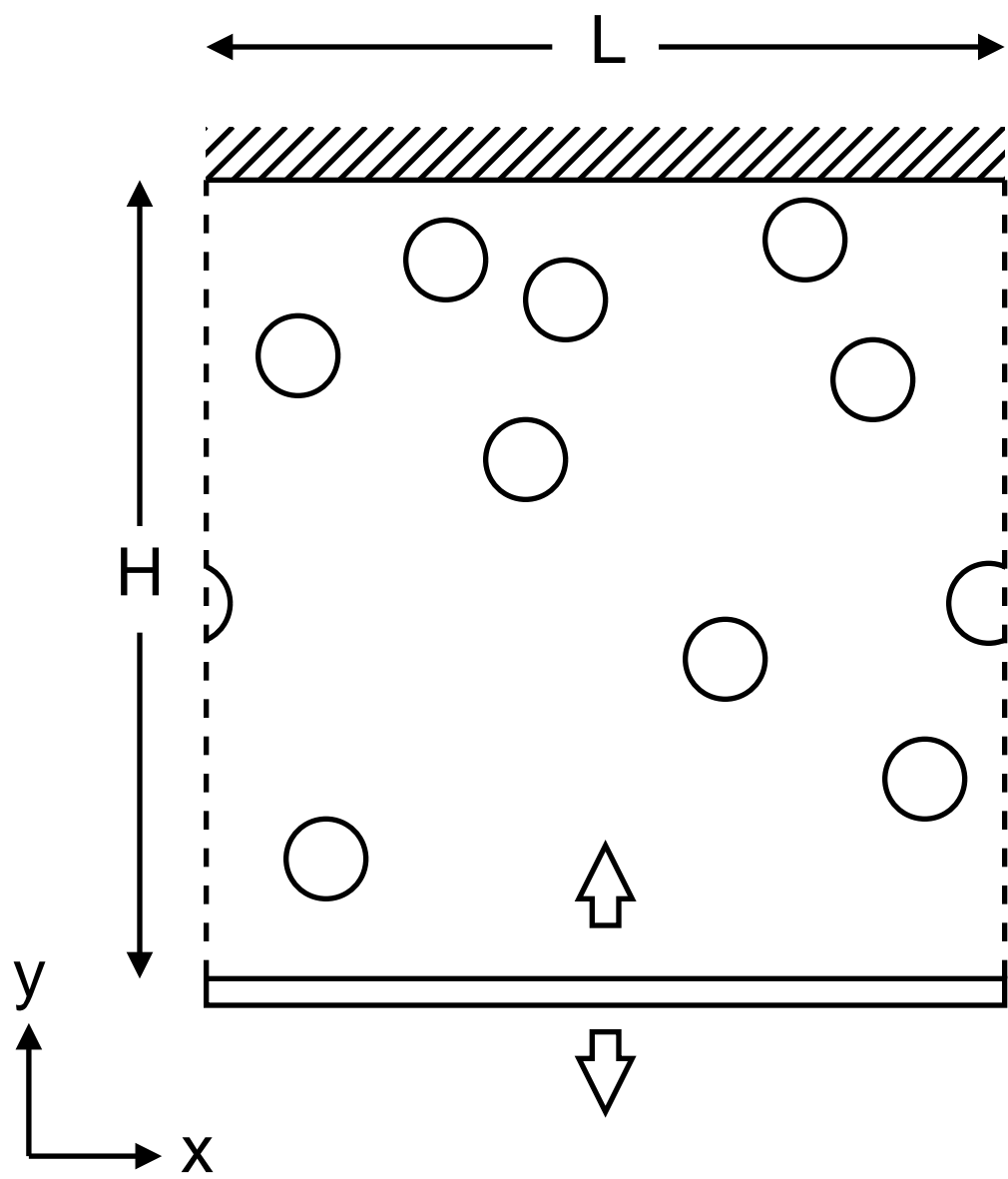
FIG. 3. Profiles of temperature (a) and density (b), (measured by the local area fraction ν). The nondimensional parameters are $L = H = 50a$, $r = 0.95$, $N\pi a^2/LH = 0.25$, $A = 2$ and the symmetric waveform. [There are about $N/(L/2a) \approx 8$ layers of particles.] In each graph, there are four lines showing the field values at four times during the driving cycle. The wall is at its lowest point ($y = 0$) at $t = 0$, and at its highest point ($y = A = 2$) at $t = 0.5$. At $t = 0.25$ ($t = 0.75$), it is halfway between these extremes, and ascending (descending).

FIG. 4. The power input scaled as $P_w = pVL F(U/V)$. The bold points were generated by the symmetric waveform; the lighter points by the asymmetric. The parameters are $L = H = 50a$, $N\pi a^2 = 0.25$, $1 \leq A \leq 5$ (as indicated on the graph), and $0.8 \leq r \leq 0.998866$.

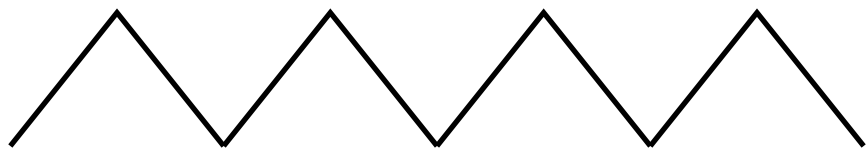
FIG. 5. The same data as the bold points in figure 4 (symmetric waveform), but scaled with the second scaling presented in the text: $P_w = (pV^2 L \tau / H) G[U \tau / (H - A)]$. The points which disobey the previous scaling collapse onto a single curve. The gap at $0.5 \leq U/(H - A) \leq 0.8$ is caused by the resonance between the sound waves and the vibrating wall. This gap corresponds to the discontinuities in figures 2 and 4.

REFERENCES

- [1] I. Goldhirsch and G. Zanetti, Phys. Rev. Letters, **70**, 1619 (1993).
- [2] S. McNamara and W.R. Young, Phys. Rev. E, **53**, 5089 (1996).
- [3] P. Deltour and J.L. Barrat, submitted to J. Physique.
- [4] S. Warr, J. Huntley, and G. Jacques, Phys. Rev. E, **52**, 5583 (1995).
- [5] S. Luding, H. Herrman, and A. Blumen, Phys. Rev. E, **50**, 3100 (1994).
- [6] J. Lee, Physica A, **219**, 305 (1995).
- [7] J. Lee, preprint.
- [8] S. Fauve, private communication.



(A)



(B)

